ELSEVIER

Cryogenics 40 (2000) 539–548

Cryogenics

www.elsevier.com/locate/cryogenics

Predictive study of current sharing temperature test in the Toroidal Field Model Coil without LCT coil using the M&M code

L. Savoldi [1], R. Zanino *

Dipartimento di Energetica, Politecnico di Torino, 24, C.so Duca degli Abruzzi, 10129 Torino, Italy

Received 1 September 2000; accepted 10 January 2001

Abstract

The Toroidal Field Model Coil (TFMC) will be tested next year at Forschungszentrum Karlsruhe, Germany, in the frame of the International Thermonuclear Experimental Reactor (ITER). The TFMC is pancake-wound on radial plates using 10 Nb_3Sn two-channel cable-in-conduit conductors, jointed on the inner- and outer-side of the coil. The drivers for the test of current sharing temperature (T_{cs}) are the resistive heaters located on the inlet plumbing to each conductor (DP1.1, DP1.2) of the first double pancake (DP1). Since all available sensors are outside the coil, T_{cs} in the conductor must be measured indirectly, which requires sophisticated analysis tools because of the complexity of the system. In the present work we use the recently developed Multi-conductor Mithrandir (M&M) code. The main aim of the paper is of assessing computationally possible scenarios of normal zone initiation in the high field region of the conductor, without quench propagation out of the inlet joint, in the test configuration without LCT coil.

Keywords: Cable-in-conduit conductors; Superconducting cables; Fusion magnets

1. Introduction

The Toroidal Field Model Coil (TFMC) [1,2] will be tested next year in the TOSKA facility of Forschungszentrum Karlsruhe, Germany, in the frame of the International Thermonuclear Experimental Reactor (ITER). This racetrack coil is pancake-wound on radial plates using 10 Nb_3Sn two-channel cable-in-conduit conductors (CICC). Conductors on the same radial plate are jointed on the inner side of the coil, while conductors on adjacent radial plates are jointed on the outer side. The helium coolant enters each conductor through the joint located on the inner side of the coil and, since the joints are of the shaking-hands type, it flows in opposite directions in each of the jointed conductors.

The TFMC will be operated both with and without the adjacent LCT coil, which is bound to it by an inter-coil structure. Among the tests foreseen in the program [3,4] we shall concentrate here on the measurement of the current sharing temperature (T_{cs}), i.e., the temperature at which the operating current $I = 80$ kA becomes the critical current, without LCT coil. Since all available sensors are outside the coil, T_{cs} must be measured indirectly, using as drivers the resistive heaters located on the inlet plumbing to each conductor (DP1.1, DP1.2) of the first double pancake (DP1). The heated helium, convected to the high field region $\sim$2 m downstream from the joint inlet, should originate there a normal zone that can be revealed by voltage taps at the conductor ends. A suitable criterion on the measured voltage will finally be used to define T_{cs} in the experiment.

In the present work, we mainly aim at assessing computationally possible scenarios of *normal zone initiation in the high field region of the conductor, without quench propagation out of the inlet joint*. The recently developed Multi-conductor Mithrandir (M&M) code [5] is applied, taking into account several issues, which may be crucial in the assessment of the experimental strategy like:

- operation scenario of the resistive heaters,
- critical properties of joint vs. conductor,
- heat exchange between half-joints,

* Corresponding author. Tel.: +39-011-564-4490; fax: +39-011-564-4499.

E-mail addresses: savoldi@polito.it (L. Savoldi), zanino@polito.it (R. Zanino).

[1] Tel.: +39-011-564-4447; fax: +39-011-564-4499.

0011-2275/01/$ - see front matter
PII: S0011-2275(01)00010-8

Nomenclature

B_{c20m}	upper critical field at $T = 0$ (T)
C_0	normalization constant for the critical current density (AT/m^2)
C_v	helium specific heat at constant volume (J/kg K)
dm/dt	helium mass flow rate (kg/m^3)
H1	heater upstream of DP1.1
H2	heater upstream of DP1.2
I	transport current (A)
M	generic manifold in the cryogenic circuit
p_{out}	helium pressure in the outlet manifold M2 (Pa)
P_J	Joule power dissipated in the joints (W)
Q_1	power input from heater H1 (W)
Q_2	power input from heater H2 (W)
Q	power deposition (W)
s	helium entropy (J/kg K)
t	time (s)
T	temperature (K)
T_{c0m}	critical temperature at $B = 0$ (K)
T_{cs}	current sharing temperature (K)
T_{st}	strand temperature (K)
x	spatial coordinate along the conductor axis (m)
W	$\min[T_{cs}^{joint}] - \min[T_{cs}^{conductor}]$ (K)

Greeks

ε_{joint}	strand strain in the joint region
$\varepsilon_{conductor}$	strand strain in the conductor region
Φ	Gruneisen parameter
ρ	helium density (kg/m^3)
τ_Q	duration of the heating plateau (s)
τ_R	duration of the ramp (s)

- non-lumped treatment of the non-externally heated pancakes in the cryogenic circuit.

The paper is organized as follows: in Section 2 we define the problem in more detail. We then present the model used for the analysis, including both the TFMC and the external cryogenic circuit, which is part of the TOSKA facility. The model is then used to analyze parametrically the scenarios, which we consider of interest. Finally, conclusions and recommendations are drawn from the results of the analysis.

2. Definition of the problem

The nature of the problem of T_{cs} measurement in the TFMC can be easily understood by considering Fig. 1. The magnetic field distribution in the direction x along each conductor, computed [6] at the inner line on the conductor cross-section, i.e., the maximum field, is shown in Fig. 1(a) for the cases of DP1.1 and of DP1.2. [2] The lap-type shaking-hands joint between DP1.1 and DP1.2 extends for about the first 0.5 m. Notice finally that although in the operation without LCT the maximum field B, i.e., the minimum T_{cs}, is in DP3.2 [6], this cannot be used because of the absence of a heater on that pancake.

If we use for the superconductor parameters the recommended values $C_0 = 1.1 \times 10^{10}$ AT/m^2, $B_{c20m} = 29.1$ T, $T_{c0m} = 16.9$ K, $\varepsilon_{joint} = -0.6\%$, $\varepsilon_{conductor} = -0.5\%$ [8], it is easy to derive from definition [9] the profile of T_{cs} along the conductor [10], which is shown in Fig. 1(b). (Notice that the discontinuity in ε leads to a discontinuity in T_{cs} at the joint/conductor transition.) A very important consequence may be drawn from Fig. 1(b): there is no practical way to initiate a normal zone in DP1.1 near the maximum field, i.e., at a relatively safely known location, by externally heating the helium. Indeed, the available "window" $W \equiv \min(T_{cs}^{joint}) - \min(T_{cs}^{conductor})$ for normal zone initiation in the conductor, without having a quench propagating in advance out of the joint, is ~0.1 K, i.e., essentially negligible from the point of view of a predictive analysis. On the contrary, $W \sim 0.4$–0.5 K for DP1.2, i.e., if helium comes in at the joint with a temperature $T \sim 9.1$ K, and does not get cooled more than 0.4 K in about 2 m travel along the conductor, a normal zone will be initiated in the conductor without quench propagation out of the joint. (In principle it would also be possible, strictly speaking, to quench the conductor without quenching the joint even entering at $T > \min(T_{cs}^{joint})$, taking advantage of the negative slope of $T_{cs}(x)$ and of the damping of the slug while it travels downstream in the joint. However, we consider this possibility as a sort of extrema ratio.)

Again from Fig. 1 one can also see that the most likely location of normal zone initiation in DP1.2 is around 1.5 m from the joint inlet, i.e., *near* the maximum field, considering that from there on the T_{cs} does not vary too much, while heat diffuses and needs time to be convected along the conductor. Finally, it is also worth noticing that, unless a significantly higher power is used to heat the helium in DP1.1 than in DP1.2, which however is not advised as seen above, the inlet temperature to DP1.1 will be lower than in DP1.2 because the mass flow rate there will be higher, which is due in turn to the fact

[2] Notice that computed magnetic field variations *on* the cross-section are up to 0.5–1 T [6], which introduces a number of principal difficulties [7]. An analysis of this feature, which is also related to the question of the distance from the joint needed for the current to redistribute uniformly on the conductor cross-section, lies beyond the scope of the present paper. Here it will then be assumed that the current density is distributed uniformly among the strands, and that the field distribution is uniform at the maximum value of the actual field.

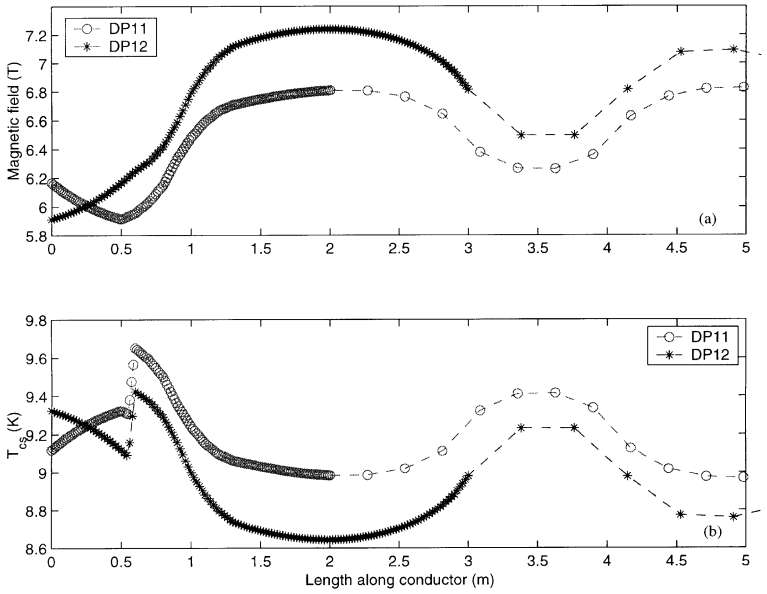

Fig. 1. Behavior of magnetic field and current sharing temperature near the inlet of the heated pancakes. (a) Spatial profile of the maximum magnetic field in pancakes DP1.1 (○) and DP1.2 (∗), computed along the conductor "inner line" [6]. (b) Spatial profile of T_{cs} in DP1.1 (○) and DP1.2 (∗), resulting from (a) using critical current parameter values $C_0 = 1.1 \times 10^{10}$ AT/m^2, $B_{c20m} = 29.1$ T, $T_{c0m} = 16.9$ K, $\varepsilon_{joint} = -0.6\%$, $\varepsilon_{conductor} = -0.5\%$ [8]. The density of the symbols gives the idea of the mesh refinement in the joint (before the discontinuity in T_{cs}) and in the following first few meters of conductor.

that DP1.1 is shorter (∼72 m) than DP1.2 (∼82 m). This will be relevant to guarantee that a normal zone is *not* inadvertently initiated in (the half-joint of) DP1.1.

In conclusion, we shall concentrate our efforts on strategies to initiate a normal zone in DP1.2. *By definition we shall assume that this happens as the conductor temperature profile intersects the T_{cs} profile* and, in particular, it will not be attempted for the time being to follow with the code the simultaneous evolution of the voltage measured across DP1.2.

3. Description of the model

The model we use is based on the M&M code [5], which incorporates a Mithrandir [11] treatment for an arbitrary number of thermally and hydraulically coupled two-channel CICC, together with the Flower [12,13] solver for the closure of the cryogenic circuit of TOSKA external to the TFMC per se. Notice that the experimental problem we are addressing is rather difficult and delicate, in view of the narrowness of W, and from the modeling point of view it requires validation of the different ingredients in the tools for analysis, with a proven accuracy corresponding to errors well below W, i.e., typically not above 0.1 K! For the Mithrandir/M&M chain of codes this was shown to be the case in previous validation exercises, as reported in a series of papers on heat slug propagation in QUELL [14,15], coupling to Flower [16], and joint thermal-hydraulics [17,18].

The actual cryogenic system of the TFMC in TOSKA is extremely complex [19]. Here we have attempted to model it as in Figs. 2(a) and (b), maintaining most of what we consider to be the essential features.

As one sees in Fig. 2(a), a volumetric pump produces a constant mass flow rate $dm/dt = 180$ g/s of supercritical helium, which is brought back by a heat exchanger to the design inlet temperature in the winding of 4.5 K. (The parallel circuits feeding the two busbars for a total of 36 g/s nominal are neglected here, for the sake of simplicity.) The plumbing up to the inlet manifold M3 is approximated by a M4 (volume = 0.1 m^3). All pancakes are connected in parallel (see below) between M3 (volume = 0.001 m^3) and M2 (volume = 0.1 m^3), the latter being kept at a constant operating pressure p_{out} (= 0.35 MPa nominally) by a couple of one-way valves + the big reservoir M5 (volume = 10^3 m^3). In the actual circuit only one valve is present, impeding that the pressure goes *below* 0.35 MPa, while the other is just a temporary artifact to mimic much more complex components, for the time being. The volume chosen for M4 comes from a very rough estimation of the helium in the hydraulic circuit of TOSKA (O(10 m) piping, where the "O" symbol indicates the order of magnitude, with inner diameter of ∼36 mm [20], plus the helium contained in the case and support structure piping), while the volume chosen for M3 comes from a very rough estimation of the helium in the TFMC before the joint inlets (O(1 m) piping with inner diameter of 10 mm for each non-heated pancake). The helium volume in M2 does not have any influence on the simulations because its

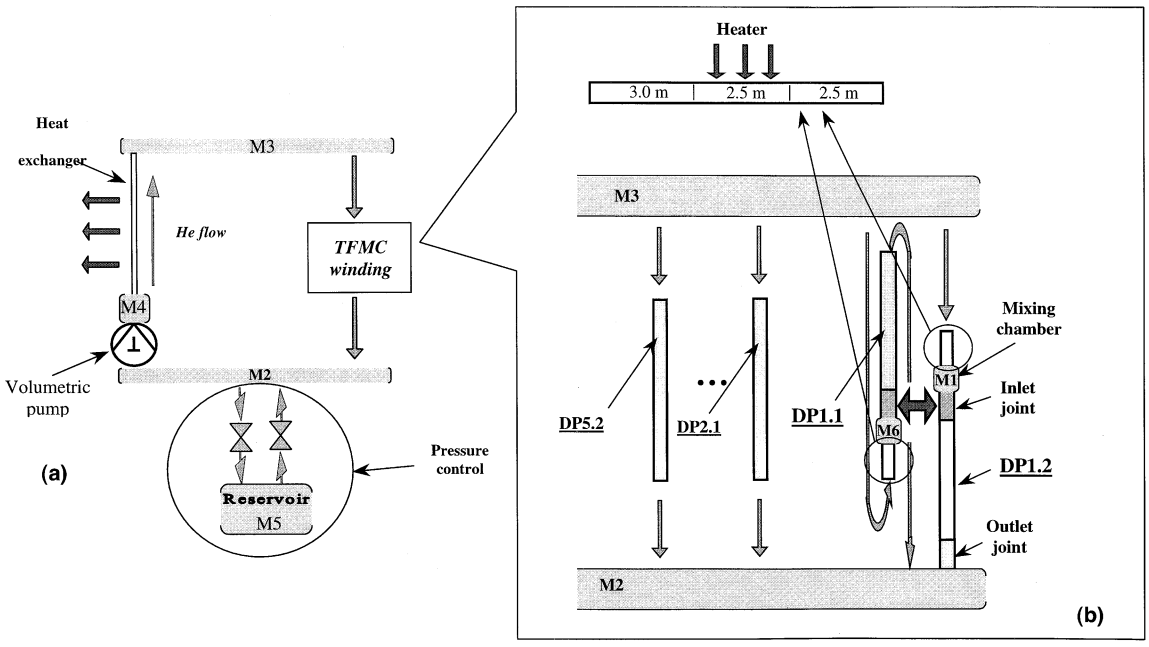

Fig. 2. Model of the cryogenic circuit used in the simulations. (a) Portion of the circuit with the volumetric pump providing a constant mass flow rate to the TFMC winding. The pressure in the outlet manifold M2 is maintained at a constant level. (b) Model of the TFMC winding. All pancakes are modeled by M&M as separate conductors, with the respective lengths and spirals (Showa, for DP1 and DP5, or Cortaillod, for DP2–DP4) delimiting the central channel [25]. For the heated pancakes DP1.1 and DP1.2 the heat exchange in the inlet joint is accounted for. The heaters at the inlet of DP1.1 and DP1.2 are also modeled with M&M and connected to the conductors through a volume, which simulates the mixing chamber at joint inlet.

pressure is kept constant, and the transients analyzed here are too short to cause significant temperature changes at the outlet of the winding.

A major novel point in this work comes with the model of the TFMC winding between M3 (inlet manifold) and M2 (outlet manifold), as shown in Fig. 2(b).

Concerning DP1, the helium flows first in the two independent 2.5 m long heaters, modeled themselves as part of 8 m long "conductors" and treated with M&M in order to provide power deposition *in the pipe*, which is not allowed in Flower; this was shown to be suitable in a separate limited validation on LCT data. Then it flows counter-current in the two inlet half-joints, through the respective mixing chambers (separately modeled by M1 and M6 with 5×10^{-5} m^3 volume [3]), and finally in DP1.1 and DP1.2. (In DP1.2 also the outlet joint is included in the model for the sake of a more accurate reproduction of the mass flow rate in this crucial pancake.) Notice that thermal coupling via the copper sole is allowed between the two half joints at the inlet of DP1.1, DP1.2 [5]. This is important when the two pancakes are asymmetrically heated, which is obvious, but also when $Q_1 = Q_2$, because of the counter-current heat exchanger nature of a shaking-hands joint. The control valves present upstream of each heater have not been included in the model for the time being, i.e., we assume for the sake of simplicity that the *total* initial mass flow rate in the TFMC winding can be regulated as needed.

Each of the other pancakes is modeled as a separate conductor, and this should constitute a significant improvement with respect to previous approaches, where either no parallel is present [22,23] or all pancakes except one are lumped into a single smooth tube [21]. First, this allows having *both* DP1.1 and DP1.2 heated, as in reality. Second, it was already shown [24] that lumping can lead to significant inaccuracies in the mass flow rate repartition in the winding *during the transient*, particularly because of the different friction features of the central channel of conductors using the Showa spiral (DP1 and DP5) or the Cortaillod spiral (DP2 to DP4) [25]. Thermal coupling between different turns of the same conductor or between adjacent pancakes on the same radial plate was neglected because it occurs on time scales, which are typically longer than those of interest here.

Finally, concerning the transport current I we adopt the following strategy for the present, essentially thermal-hydraulic study: we obviously consider I for magnetic field generation and additionally for Joule heat generation P_J in the joints, but if the conductor temperature reaches the T_{cs} at some point, no quench is

[3] Notice that this little volume more or less exactly corresponds to the actual size of the mixing chamber. Unfortunately, M1 and M6 cannot be modeled with a significantly larger volume, which would allow a larger time step to be used by Flower, because this would distort the crucial temperature waveform at the joint inlet. The alternative of modeling the whole heater+joint+conductor set as a single conductor [21] was not pursued here.

initiated and the run proceeds normally up to the end as defined in the input file. It may be considered that *this strategy attempts to mimic purely thermal-hydraulic tests, which should take place before the T_{cs} tests themselves* [3], with the additional ingredient of P_J, which will be relevant for the actual T_{cs} runs.

4. Results and discussion

The set of experimentally available control parameters to achieve our target, subject of course to the constraints from the refrigeration system capacity [19], can be roughly listed as follows:

- Heating scenario (≡ time shape of heater power generation):
  - heat slug (i.e., approximately square wave of given amplitude Q and duration τ_Q),
  - ramp (of given final amplitude Q and duration τ_R),
  - step (≡ ramp of given final amplitude Q and duration τ_R followed by plateau of given duration τ_Q, possibly multiple),
  - independent use of the two heaters H1 on DP1.1 and H2 on DP1.2,
- Initial mass flow rate in the TFMC winding.
- Outlet pressure from the TFMC winding.

Notice that the constraint on the maximum available refrigeration capacity of about max 500 W for 300 s [26] excludes in the TFMC the practicability of the quasi-steady strategy ($\sim 10^4$ s long series of steps with Q up to 500 W) recently used for the same purpose on the CSMC [27].

We shall start with the analysis at nominal operating conditions of 18 g/s/pancake mass flow rate and 0.35 MPa outlet pressure from the TFMC winding. These parameters will then be varied. In all cases conductor geometry is defined in [28] while joint data are given in [29].

4.1. Analysis at nominal operating conditions

As suggested in several TFMC Test Group and Test & Analysis Meetings, we started our study considering the heat slug scenario (actually, ramp up and down with a very short duration $\tau_R = 1$ s, separated by a plateau of τ_Q s), with the same power shape in both heaters. All of the tested heat slug runs led to either no normal zone initiation or to quench propagation out of the joint accompanied by *large oscillations in time of the inlet temperature, whenever the temperature attempted to rise above* ~7 K. A similar behavior was observed with ramp and with step scenarios.

As a case representative of "typical" results at the nominal pressure of 0.35 MPa we show in Figs. 3(a) and (b) the results of the analysis for a step with $Q_1 = Q_2 = 275$ W (i.e., 550 W total), ramp duration $\tau_R = 40$ s and plateau duration $\tau_Q = 20$ s. Notice that a minimum τ_Q, O(10 s), is required for the helium to heat the surrounding materials and then be convected from the heater exit to the maximum field region, mainly with unperturbed temperature peak except for heat exchange between and heat generation in the two half joints. On the other hand, the choice of the values of Q, τ_R and τ_Q is not specifically relevant for the case at hand, but it will become useful for subsequent comparisons, see below. Conditions at the inlet *of the joint* to each of the two heated pancakes are reported.

It may be observed from Fig. 3 that, in the first phase of the transient, i.e., while the temperature is still "sufficiently" low, the effect of the heating is to increase the temperature (which is obvious) and to reduce the mass flow rate, *in the heated pancakes*. In the second phase of the transient, large oscillations start both in the temperature and in the mass flow rate (notice that the latter are small in absolute terms but large in relative terms).

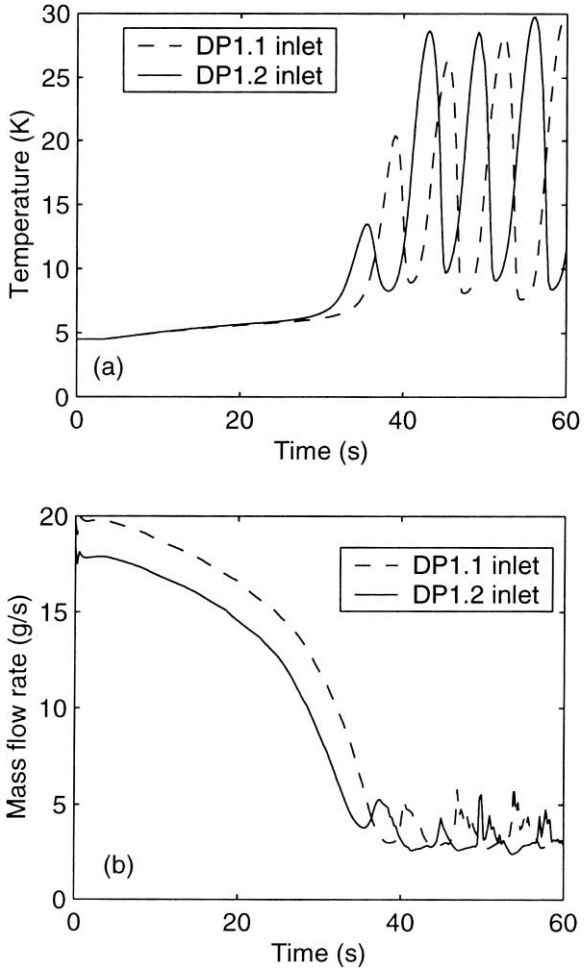

Fig. 3. Results for the symmetrical heating scenario with $Q_1 = Q_2 = 275$ W, ramp with $\tau_R = 40$ s duration followed by a plateau with $\tau_Q = 20$ s duration. Fixed outlet pressure $p_{out} = 3.5$ bar. (a) Time evolution of the helium inlet temperature in DP1.1 (dashed) and DP1.2 (solid). (b) Time evolution of the helium inlet mass flow rate in DP1.1 (dashed) and DP1.2 (solid).

Let us begin explaining the first part of the transient, assuming the heater power would have actually reached its plateau without oscillations, so that a new steady state would be reached. As a consequence of the heating, the pressure in the inlet manifold increases to a new value. Since the outlet pressure is constant, the pressure drop across the parallel is increased in the new steady state [30], and it will compensate a new value of the friction term, which is proportional to $(\mathrm{d}m/\mathrm{d}t)^2/\rho$. Since the temperature at the inlet of the non-heated pancakes is always constant at 4.5 K, the density there will at most increase a bit because of the pressurization, therefore $(\mathrm{d}m/\mathrm{d}t)$ will have to increase in the non-heated pancakes. This will cause a reduction of the mass flow rate in the heated pancakes, as observed in Fig. 3(b), because the volumetric pump forces in the new steady state always the same total mass flow rate as before heating.

Coming now to the oscillations, we first of all excluded their numerical origin by a convergence study. It is quite obvious a priori that oscillations would not be acceptable from the point of view of the tests, considering the above-mentioned sensitivity to variations of a few tenths of a Kelvin, so that, they are worth a more detailed investigation. Notice also that so-called "density waves", which appear to have very similar features to what we see in our simulations, have been actually observed in experiments on the LHC beam screens, where a weakly supercritical He flow is used to intercept most of the dynamic heat load [31]. However, while in [31] the inlet flow is *assumed* to be oscillatory, we shall attempt to find here a self-consistent qualitative explanation of the phenomenon, based as in [31] on the weakly supercritical state of the helium.

In order to understand the possible "physical" origin of the oscillations in our model, let us begin by observing that, for a given energy input Q, the increase in temperature and the pressurization are, respectively [5],

$\partial T/\partial t$ proportional to $Q/(\rho C_\mathrm{v})$,

$\partial p/\partial t$ proportional to $Q * \Phi$,

where $\Phi \equiv (\rho/T)(\partial T/\partial \rho)_s$ is the Gruneisen parameter. The two coefficients of proportionality are given in Figs. 4(a) and (b), respectively, for two different pressures. It is clear that although at 0.35 MPa we are operating at supercritical pressure, the variation of the thermodynamic properties with temperature is still strong enough when helium crosses the pseudo-critical line. As a consequence of this, and with reference to the model of the hydraulic circuit shown in Figs. 2(a) and (b), we can imagine the following chain of events leading to the oscillations: once the temperature starts approaching the pseudo-critical line, near 6–7 K, the still increasing Q causes a "quadratic" increase of the temperature, because of the strong decrease of ρC_v, which explains the change of slope near $t \sim 30$ s in Fig. 3(a). Simultaneously, the pressurization under the heater is being reduced, because of the strong decrease of Φ. Since the volume of the inlet manifold M3 is finite, its pressurization cannot follow instantaneously the heater region, so that the increasing pressure gradient between inlet and heater causes a reduction in the decrease of mass flow rate in heated pancakes, and an eventual increase of it, as seen in Fig. 3(b). This leads to a decrease of the temperature, and therefore to a re-pressurization of the helium under the heater, and so on. Notice that small errors in the helium volume estimation in M3 have been shown numerically not to affect the oscillations.

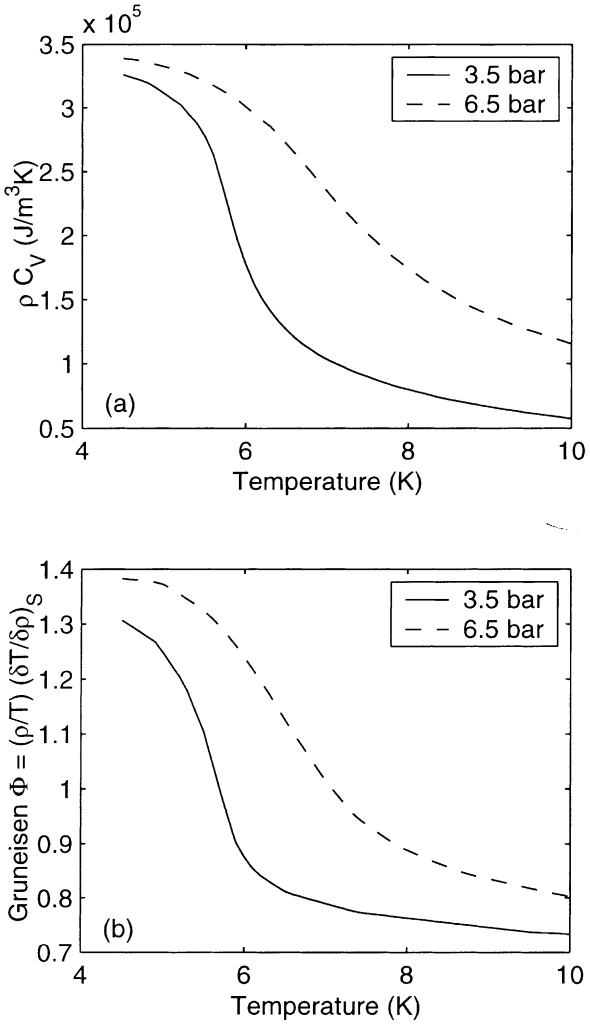

Fig. 4. Thermodynamic properties of helium as a function of helium temperature, for different pressures. (a) Product of helium density ρ and specific heat C_v, computed at 0.35 MPa (solid) and 0.65 MPa (dashed). (b) Gruneisen parameter Φ, computed at 0.35 MPa (solid) and 0.65 MPa (dashed).

The period of the oscillations can be related to the time needed for convection of the helium in the 8 m long heated pipe. From this point of view it may be observed that the 3 m long pipe included upstream of the heater in the model of Fig. 2 corresponds in reality to O(1 m) piping plus a control valve, while the 2.5 m long pipe

downstream corresponds to the actual piping length. The effect of the actual circuit on the oscillations should therefore be checked, in particular with respect to the portion *upstream* of the heater and, possibly, to the pressure control at the outlet manifold.

The previous considerations, together with the comparison of the gas behavior at different pressures shown in Fig. 4, lead us therefore to *analyze new test conditions, where the operating pressure is increased to, say, 0.65 MPa*. This pressure increase would still be allowed by the facility, limited to the test configuration without LCT coil [26]. The advantage of this should be to have (1) a reduced slope in the transition though the pseudo-critical line, i.e., smaller amplitude of the oscillations if any, and (2) the transition at a higher temperature, i.e., a wider operation range available for the heaters. Notice also that, at least in the case without LCT coil, operation at an increased pressure should also be feasible in practice, respecting the constraints from the refrigeration system [26].

4.2. Analysis at increased outlet pressure

In the case of heat slugs (i.e., $\tau_R = 1$ s), some oscillations still appear in the solution, although significantly smaller than in corresponding cases at 0.35 MPa. In an attempt to control them we started considering steps [4] with $Q_1 = Q_2$, but increasing τ_R to 10, 20, 40 s, while always keeping $\tau_Q = 20$ s for the above-mentioned reasons. In the last case, presented in Figs. 5 and 6, the very same operating conditions as in Fig. 3 apply, except for the increase in the pressure at the outlet manifold M2, and in the following this case will be referred to as "reference case".

In Fig. 5 we notice first of all that the large O(10 K) oscillations, which were present at lower pressure, have now reduced to O(0.1 K). In Fig. 6(b) we then see that this heating strategy leads in the simulation to a normal zone initiation somewhere between DP1.2 conductor inlet and maximum field (actually, not shown, at ~1.5 m from the inlet), without quench propagation out of the inlet joint, see Fig. 6(a). At the time (~10 s after beginning of the plateau) when the T_{cs} is reached in the

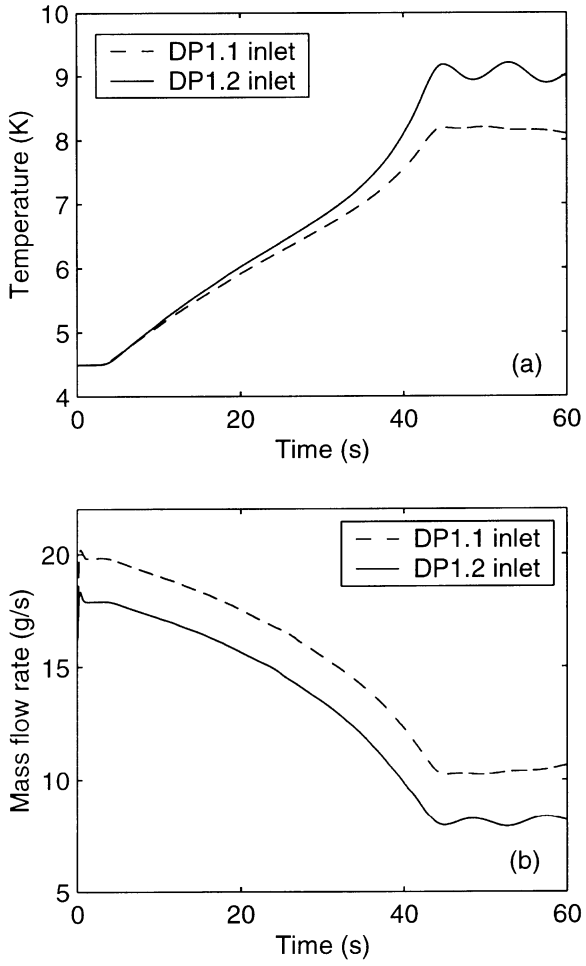

Fig. 5. Results for the symmetrical heating scenario with $Q_1 = Q_2 = 275$ W, ramp with $\tau_R = 40$ s duration followed by a plateau with $\tau_Q = 20$ s duration. Fixed outlet pressure $p_{out} = 0.65$ MPa. (a) Time evolution of the helium inlet temperature in DP1.1 (dashed) and DP1.2 (solid). (b) Time evolution of the helium inlet mass flow rate in DP1.1 (dashed) and DP1.2 (solid).

DP1.2 conductor, the minimum temperature margin in the joint is ~0.2 K, which gives again an idea of the accuracy requested to this type of calculation. In view of the fact that only the inlet and outlet temperatures would be experimentally available for an estimate of T_{cs}, we may finally observe that, in the case at hand, the computed inlet and outlet temperatures reached at T_{cs} are 9.0 and 4.5 K, respectively, while the computed T_{cs} is 8.7 K. It may be noticed that, at least with the present strategy, the damping of the heat pulse between inlet and peak field region is few tenths of a Kelvin, so that the inlet temperature measurement would give a rough estimate of the experimental T_{cs}.

Considering the above-mentioned needed accuracy, we have attempted a limited assessment of the sensitivity of our result to a few parametric effects, which may be of interest for the test, with reference to the list of control variables discussed previously. The results are summarized in Table 1.

[4] For the present we have not considered ramps at 0.65 MPa. Steps appear to be in themselves more attractive, because they lead to more steady state, i.e., more controlled conditions. Furthermore, for a given step scenario among those presented here, i.e., with relatively large dQ/dt, the corresponding ramp (i.e., further increase of the power Q with the same dQ/dt, without plateau) could only increase the chance of a quench propagating out of the inlet joint, before a normal zone is initiated in the conductor. Indeed, the constraint on dQ/dt is that it should be slow enough, not to give too large a temperature increase at the joint, in the time requested by the previously heated colder helium to reach peak field (resulting in max $dQ/dt \propto (dm/dt)^2$). However, much slower ramps are more likely to violate the constraints from the refrigeration system, which become even tighter at higher pressure than nominal [26].

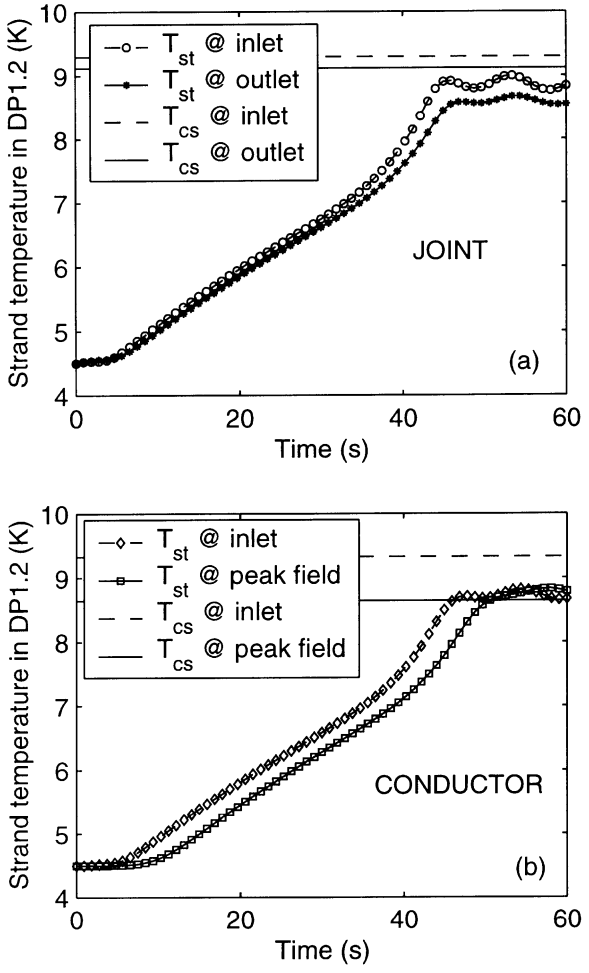

Fig. 6. Results for the symmetrical heating scenario with $Q_1 = Q_2 = 275$ W, ramp with $\tau_R = 40$ s duration followed by a plateau with $\tau_Q = 20$ s duration. Fixed outlet pressure $p_{out} = 0.65$ MPa. (a) Time evolution of DP1.2 strand temperature at the *joint* inlet (◯) and outlet (∗), compared to T_{cs} at the joint inlet (dashed) and outlet (solid), respectively. (b) Time evolution of DP1.2 strand temperature at the *conductor* inlet, i.e., at joint outlet, (◇) and at the location of peak magnetic field in the conductor (□), see Fig. 1a, compared to T_{cs} at the conductor inlet (dashed) and at peak field in the conductor (solid), respectively.

Concerning the power sensitivity, it appears from Table 1 that the window for attaining our target is rather small. As a hint of a possible practical strategy, trapezoidal pulses based on the steps just analyzed could be tried with increasingly larger Q, starting from a "safe" value. An alternative strategy could be to further increase the power in very small steps, after a plateau at given power leads to no normal zone initiation. Here we have made until now a very limited attempt to analyze the latter multiple-step strategy, which however includes also some subtle effects on the transit time scale of helium in the conductor, which will not be discussed in detail here. For example, if one increases Q, e.g., from 260 to 290 W in steps of 5 W, no normal zone is initiated anywhere, as opposed to a direct step to 290 W (see Table 1) which leads to quench propagation out of the inlet joint. This appears to be related to the mass flow behavior in the heated pancakes, which starts increasing again, on average, leading to an average decrease of the temperature notwithstanding the increase of Q. We plan to analyze the whole strategy in more detail in the future.

Finally, a degree of freedom to take advantage of would be, as mentioned above, to operate the two heaters H1 and H2 with different powers. The reason of interest for this strategy is to use the increased cooling resulting from heat conduction through the inlet joint to the colder (less-heated) conductor. This should allow having colder strands in the joint, while most of the hot helium flows in the relatively thermally isolated central channel (3 mm thickness, not perforated), allowing then the possibility to initiate the normal zone in the conductor after the perforated spiral starts delimiting the central channel, passed the end of the joint. It may be interesting to notice that this qualitatively expected feature is actually observed both in the experiment [5] and in the present simulations, see, e.g., Fig. 7(a). Another less obvious and possibly interesting feature appears in this case, namely that, all other conditions being equal except $Q_1 = 0$, the flow reduction in DP1.2 is significantly smaller than with $Q_1 = Q_2$, compare Fig. 7(b) with Fig. 5(b). This is due to the fact that, since one is heating in one pancake only, the pressurization of M3 will be lower, i.e., the mass flow increase in the non-heated pancakes will be lower, and for constant total mass flow in the TFMC winding this will force a lower reduction of the mass flow in DP1.2. For the present we have only attempted runs with power $Q_1 = 0$ in H1, see Table 1. It appears that the operation point of interest for us, if present, needs further refinement of the input power, and/or an extension of this strategy by using $Q_1 \neq 0$ while still keeping $Q_1 \neq Q_2$.

5. Conclusions and perspective

We have analyzed with the M&M code possible scenarios for T_{cs} measurement in the TFMC without LCT coil, to be performed next year at FZ Karlsruhe, Germany. A fairly sophisticated model of the TFMC winding has been developed and used, which is the major novel ingredient in the present work.

At the nominal operating pressure of 0.35 MPa oscillations in time arise in the inlet temperature and mass flow rate of the heated conductors DP1.1 and DP1.2, whenever one attempts to sufficiently increase the input power, leading to quench propagation out of the inlet joint. These oscillations are not a numerical artifact, and a qualitative explanation for them was provided. While oscillations of similar nature were already observed in the LHC beam screens cooled by weakly supercritical helium, purely thermal-hydraulic tests, preceding the T_{cs} tests, will be needed to assess if this effect is real also in

Table 1
Summary of results for step heating scenario at $p_{M2} = 0.65$ MPa

Step parameters				$(dm/dt)_0$ (g/s) in DP1.2	Output[a]
Q_1 (W)	Q_2 (W)	τ_R (s)	τ_Q (s)		
275	275	40	20	18	C
275	275	20	20	18	C/O
275	275	10	20	18	J/O
290	290	40	20	18	J
260	260	40	20	18	N
275×2/3	275×2/3	40	20	12	C/O
275×1/2	275×1/2	40	20	9	N/O
275×1/2	275×1/2	40	30	9	J/O
0	⩽325	40	30	9	N
0	350	40	30	9	J/O

[a] O = Oscillations O(0.1–1 K) in time are present in the solution; C = Normal zone initiated in conductor; J = Quench propagation out of inlet joint; N = No normal zone initiation.

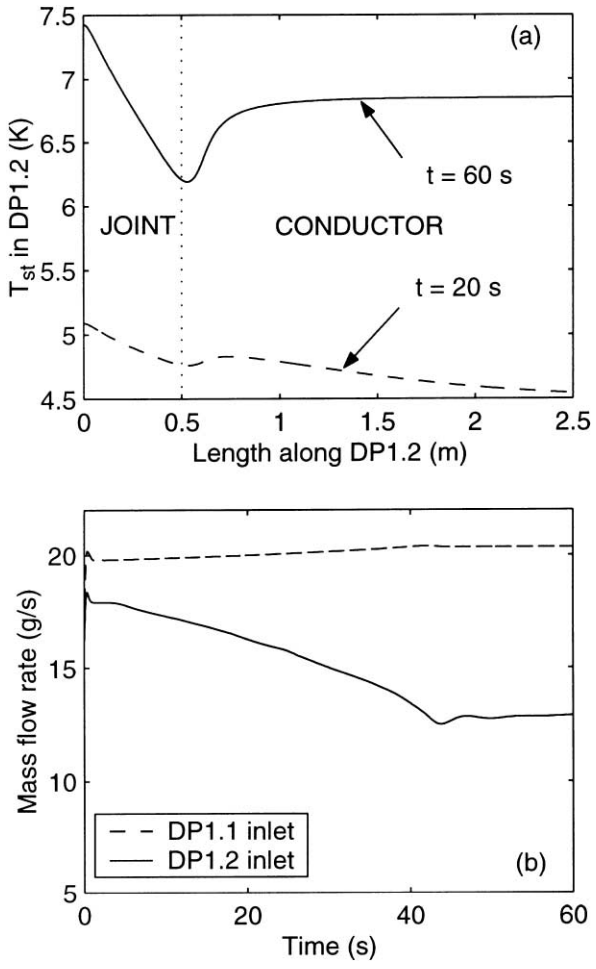

Fig. 7. Results for the asymmetrical heating scenario with $Q_1 = 0$ W, $Q_2 = 275$ W, ramp with $\tau_R = 40$ s duration followed by a plateau with $\tau_Q = 20$ s duration. Fixed outlet pressure $p_{out} = 0.65$ MPa. (a) Spatial profile of DP1.2 strand temperature at $t = 20$ s (dashed) and $t = 60$ s (solid), zoomed near pancake inlet, including joint region (∼first 0.5 m) and conductor inlet region (following 2 m). (b) Time evolution of the helium inlet mass flow rate in DP1.1 (dashed) and DP1.2 (solid).

the TFMC or only a feature of the model, which is necessarily approximated.

In order to overcome this difficulty, and based on the role that the crossing of the helium pseudo-critical line has on the phenomenon, we have increased the operating pressure to 0.65 MPa in the simulations, which led in otherwise comparable cases to the strong reduction of the amplitude of the oscillations. Step heating scenarios have been analyzed and it has been shown that it is possible in the simulation to initiate a normal zone in the DP1.2 conductor, without quench propagation out of the inlet joint, as desired in the tests. In case the pretests at 0.35 MPa should reveal the onset of oscillations, we should like to recommend therefore an increase in the operation pressure to, e.g. 0.65 MPa.

In perspective this analysis should be extended to include different operating currents in the TFMC, both without and with the LCT coil, as foreseen in the test program [3].

We also plan to implement and validate a suitable model for resistive voltage and power generation in the coil during T_{cs} tests. This will allow extending the present analysis to a quantitative study of quench initiation and propagation in the TFMC.

Acknowledgements

The European Fusion Development Agreement (EFDA) and the Italian Ministry for University and Scientific and Technological research (MURST) have partially financially supported this work. We also wish to thank G. Zahn, F. Wuechner and R. Heller for a number of discussions and information on the TOSKA/TFMC cryogenic system, for providing the original drawings of the TOSKA/TFMC and for LCT data. We kindly acknowledge the useful and stimulating input coming from the contributions of several colleagues regularly participating to the TFMC Test and Analysis

Meetings, among which H. Fillunger, J.-L. Duchateau, D. Ciazynski, C. Marinucci, A. Martinez, P. Hertout, and A. Ulbricht. Finally, we wish to thank Ph. Lebrun for pointing out [31] to us.

References

[1] Salpietro E. ITER toroidal field model coil (TFMC) design and construction. Fus Technol 1998;34:797.
[2] Komarek P, Salpietro E. The test facility for the ITER TF model coil. Fus Eng Des 1998;41:213.
[3] Ulbricht A. Draft of TFMC test procedure without and with LCT coil, September 2000 (unpublished).
[4] Duchateau J-L, et al. Test program preparations of the ITER toroidal field model coil (TFMC). In: Presented at the 21st Symposium on Fusion Technology. Madrid, Spain; 2000 September 11–15.
[5] Savoldi L, Zanino R. M&M: Multi-conductor Mithrandir code for the simulation of thermal-hydraulic transients in superconducting magnets. Cryogenics 2000;40:179.
[6] Hetrout P. Magnetic field calculations for the ITER toroidal field model coil. CEA Report, AIM/NTT-1999.048.
[7] Mitchell N. Steady state analysis of non-uniform current distributions in cable-in-conduit conductors and comparison with experimental data. Cryogenics 2000;40:99.
[8] Ciazynski D. Evaluation of Nb_3Sn strain in the three EU FSJS's (conductor and joints): application to ITER TF coils and ITER TFMC. In: Presented at the 10th TFMC Test and Analysis Meeting. Cadarache, France; 1999 December 16.
[9] Summers L, et al. A model for the prediction of Nb_3Sn critical current as a function of field, temperature, strain and radiation damage. IEEE Trans Magn 1991;27:2041.
[10] Martinez A. Quench triggering by resistive heater. In: Presented at the Sixth TFMC Test and Analysis Meeting. Cadarache, France; 1998 November 19.
[11] Zanino R, De Palo S, Bottura L. A two-fluid code for the thermohydraulic transient analysis of CICC superconducting magnets. J Fus Energy 1995;14:25.
[12] Bottura L, Rosso C. Hydraulic network simulator model, Internal Cryosoft Note, CRYO/97/004, 1997.
[13] Marinucci C, Bottura L. The hydraulic solver Flower and its validation against the QUELL experiment in SULTAN. IEEE Trans Appl Supercond 1999;9:616.
[14] Zanino R, Marinucci C. Heat slug propagationin in QUELL. Part I: experimental setup and 1-fluid GANDALF analysis. Cryogenics 1999;39:585.
[15] Zanino R, Marinucci C. Heat slug propagation in QUELL. Part II: 2-fluid MITHRANDIR analysis. Cryogenics 1999;39:595.
[16] Savoldi L, Bottura L, Zanino R. Simulations of thermal-hydraulic transients in two-channel CICC with self-consistent boundary conditions. Adv Cryo Eng 2000;45:697.
[17] Zanino R, Santagati P, Savoldi L, Marinucci C. Joint+conductor thermal-hydraulic experiment and analysis on the full size joint sample using MITHRANDIR 2.1. IEEE Trans Appl Supercond 2000;10:1110.
[18] Zanino R, Savoldi L. Test and modeling of heat generation and heat exchange in the full size joint sample. In: Proceedings of ICEC 18. Mumbai, India; 2000 February 21–25. p. 363.
[19] Ulbricht A. TOSKA facility, Chapter 3 of the TFMC Summary Report, 2001, to appear.
[20] Marinucci C. Preliminary quench initiation analysis of the TFMC. In: Presented at the Ninth TFMC Test and Analysis Meeting. Karlsruhe, Germany; 1999 October 27.
[21] Marinucci C, Bottura L. Predictive quench initiation analysis of the ITER TF model coil. In: Proceedings of ICEC 18. Mumbai, India; 2000 February 21–25. p. 173.
[22] Heller R, Duchateau JL, Nicollet S, Prat F. Numerical evaluation of the quench behaviour in the ITER Toroidal Field Model Coil. Adv Cryo Eng 1998;43:189.
[23] Heller R. Quench analysis for safety purposes. In: Presented at the 11th TFMC Test and Analysis Meeting. Karlsruhe, Germany; 2000 March 20.
[24] Savoldi L, Zanino R. Heat slug injection in the TFMC (M&Mcode development). In: Presented at the 11th TFMC Test and Analysis Meeting. Karlsruhe, Germany; 2000 March 20.
[25] Zanino R, Santagati P, Savoldi L, Martinez A, Nicollet S. Friction factor correlation with application to the central cooling channel of cable-in-conduit conductors for fusion magnets. IEEE Trans Appl Supercond 2000;10:1066.
[26] Zahn G. Private communication, 2000.
[27] Savoldi L, Zanino R. Thermal-hydraulic analysis of T_{cs} measurement in conductor IA of the ITER Central Solenoid Model Coil. Cryogenics 2000;40:593–604.
[28] Nicollet S, Duchateau JL, Fillunger H, Martinez A, Parodi S. Dual channel cable in conduit hermohydraulics: influence of some design parameters. IEEE Trans Appl Supercond 2000;10:1102.
[29] Ciazynski D, Duchateau J-L, Schild T, Fuchs AM. Test results and analysis of two European full-size conductor samples for ITER. IEEE Trans Appl Supercond 2000;10:1058.
[30] Sugimoto M, Kato T, Isono T, et al. Flow reduction by AC losses for a forced flow superconducting coil with a cable-in-conduit conductor. Cryogenics 1999;39:323.
[31] Hatchadourian E. Stability and control of supercritical helium flow in the LHC circuits, Adv Cryo Eng 2000;45, to appear.